Recovery of Methyl Green from Aqueous Solution using NF Membrane

P. Sharma[1], M. M. Bora[2], S. Hazarika[3], S. Borthakur[4], C. Tamuli[5] & N. N. Dutta[6*]

[1-6]Chemical Engineering Division, NEIST, Jorhat, Assam, India

ABSTRACT

Recovery of a cationic synthetic dye, methyl green by nanofiltration (NF 270-400) membrane from commercial source (Filmtec, USA) was used for this study. The effect of membrane characteristics, applied pressure gradient (ΔP) and aqueous phase concentration of dye on the rejection, membrane fouling and water flux was studied over a range of pressure and concentration of 2 to 5 bar and 0.01 mmole L^{-1} to 0.05 mmole L^{-1} respectively. The solution flux increases with pressure in the pressure range studied indicate the effect of concentration polarization is not significant in this range. The cation shield effects of the dye on the negatively charged polyamide membrane perhaps result in decrease of permeate flux with concentration. The permeation phenomenon has been analyzed on the basis of pore flow transport model and the data analysis revealed that adsorption of dye on the membrane surface and intrinsic membrane resistance control the permeate flux.

Keywords: Methyl green, NF membrane, pore flow model, adsorption, permeability, flux

1.0 INTRODUCTION

Contamination of water resources by many organic pollutants is a major concern of global environmental pollution over the years among which dye represents one of the major polluting groups. The two major sources of dye pollution are textile and dye manufacturing industries. Large quantity of aqueous waste and dye effluents are discharged from these industries with strong persistent of colour which is environmentally unacceptable. Many of these dyes are toxic and even carcinogenic. EPA standard for dye concentration in polluted water is 550 mg L^{-1}[1]. Therefore, decolourization of the dye effluent is necessary before discharging.

A range of conventional treatment technologies such as trickling filter, active sludge, chemical coagulation, carbon adsorption, photodegradation etc. has been studied extensively for dye removal over the years [2]. Membrane technologies have drawn special attraction in this regard due to its high selectivity, high performance and cost effectiveness [3, 4]. Several authors have showed the possibility of concentrating dyes using different types of membrane (Table 1). Nanofiltration has the advantage of retaining relatively small organic molecules and bivalent ions from aqueous waste solutions which may be useful for application in the treatment of dye effluents [4]. In this study, we report a comprehensive study on nanofiltration membrane for removal of a commercially important dye from aqueous solution and an analysis of the transport mechanism of the membrane process through a modeling and simulation approach.

---
* *Corresponding to:* N. N. Dutta (email: nndutta@rediffmail.com)

Table 1 Some references on nanofiltration of dyes

Reference	System		Variables studied	Inference
Akbori et al [5] (2002)	Dye type Acid red 4 Acid orange 10 Basic blue 3 Direct yellow 8 isperse red 80 Disperse blue 56 Reactive orange 16	Membrane Desal 5DK (NF)	Effect of pH, solution concentration and salt effect on flux and retention of dyes	For anionic dye, membrane suffered from flux decline.For cationic dyes, the influence of Donan exclusion was clearly observed; membrane was not suitable for cationic dyes.
Hassani et al [6] (2008)	Cyanine 5R Red E3B Direct red 105 Carmozin 206	NF 90 4040	Evaluation of colour, COD and TDS removal by nanofiltration of dye-salt mixtures solutions produced by textile industry	Permeate flux increases with and decreases with concentration.At high concentration, flux decline took place. COD was completely removed by nanofiltration.
De Souza et al [7] (2009)	Different types of dye effluents	NF, UF and RO polymeric membrane	Permeate flux, colour reduction, turbidity and COD were evaluated	Each membrane has distinct values for permeate flux, colour, conductivity and COD reductions due to the particular chemical nature of the membrane and Molecular weight cut off (MWCO)
Gomes et al [4] (2006)	Acid orange 7	NF45	Effect of pressure, cross-flow velocity and dye concentration on permeation	
Banerjee et al [8] (2006)	Eosin dye	NF membrane of MWCO=400, Fenton's reagent	Combination of oxidation and nanofiltration	The main factor causing flux decline is adsorption Combination of oxidation and nanofiltration is more effective.
Aseeri et al [9] (2006)	Acid red 114	NF membrane(Spiral wond)	Effect of NaCl concentration on the dye removal in synthetic coloured wastewater	Better results in dye removal were achieved in presence of NaCl.
Aydiner et al [10] (2010)	Tartrazine	FM NP010 (NF)	Mass transport, membrane fouling and flux decline	Flux decline is directly related with the porosity or water permeability of the gel at the membrane gel at the membrane gel interface as a result of pore entrances and bridging of dye aggregates over the pore openings.
Chakraborty et al [11] (2004)	Textile industry ef	polyamide composite membrane (NF)	Prediction of permeate flux and permeate concentration	Concentration polarization cause flux decline. Experimental data of cross–flow nanofiltration was successfully explained by film theory.

1.1 Theoretical Aspects

Current state of knowledge on the transport mechanism of NF membrane probably supports the use of a "hybrid" models in which some parameters from the "pore-flow model" are to be considered. Accordingly, the model describes the performance of a pressure driven membrane process, ie nanofiltration, in terms of solvent flux, J_v proportional to the effective applied pressure $(\Delta P - \Delta \Pi)$ as given in equation (1)[4].

$$J_v = L / p(\Delta P - \Delta \Pi) \qquad (1)$$

where ΔP is the applied pressure (bar) across the membrane, $\Delta \Pi$ is the osmotic pressure (bar) across the membrane and can be estimated from Van't Hoff equation L/ps the solvent permeability coefficient (cms^{-1} bar^{-1}).

However, the permeation process is believed to be controlled by any or all of the mechanistic phenomenon, i.e. adsorption, fouling and osmotic flux and the flux may be represented by the membrane transport model developed by Tu et al [12] according to which

$$J_v = \frac{(\Delta P - \Delta \Pi)}{\mu R_t} \qquad (2)$$

where R_t is the total resistance of flow- $R_m + R_g + R_{ads}$. R_m represents the intrinsic membrane resistance, R_g represents the resistance due to fouling or concentration polarization and R_{ads} represents the resistance due to adsorption of the solute on the membrane. The permeability coefficient, Lp$'$ is defined as The value of R_m is calculated from the pure water permeability coefficient $L_p = 1 / \mu R_m$ with μ as the viscosity [4].

2.0 EXPERIMENTAL

2.1 Materials

The commercial membranes (FilmTec NF 270-400) were used (gift sample on request). According to the manufacturer, these membranes are polyamide thin-film composite membrane viable for operation at pH from 3-10 and temperatures up to 45°C. Polyamide compounds have amide and carboxyl groups bound to the aromatic rings, which tend to reduce membrane hydrophobicity.

Methyl green was used as the dye sample which was purchased from Sigma-Aldrich, India. Deionized water was used as the solvent throughout the experiment.

2.2 Characterization of the Membrane

The membrane was characterized for pore size, porosity, surface morphology and functional groups of polymer. Pore size and surface morphology of the membrane was determined with a scanning electron microscope (Model: JSM 6390 LV (JEOL)). FTIR spectra was recorded in a Perkin Elmer 2000 (640 B) spectrometer.

Porosity of the membrane was measured by immersing the membrane into n-butanol for 3 hours and weighing the membrane after adsorption of the n-butanol. The porosity was then calculated by the following equation

$$P(\%) = \frac{M_b / \rho_b}{M_b / \rho_b + (M_p / \rho_b)} \qquad (3)$$

where M_b is the weight of adsorbed n-butanol, ρ_b is the density of n-butanol, M_p is the weight and ρ_p is the density of the membrane material.

The pure water permeability co-efficient L_p is determined by plotting water permeability, J_w-versus pressure. The slope of the straight line gives the value of L_p.

2.3 Nanofiltration Experiments

A membrane of effective surface area of 4.53 cm^2 was used. Permeation experiments were conducted at constant temperature, 30°C with transmembrane pressure, ΔP ranging from 2 to 5 bar and a flow rate of 50 ml minute^{-1}.

Before conducting the experiments with methyl green solution, water permeability of the membrane was evaluated at each pressure. For this, deionized water was passed through the membrane with constant flow rate (50 ml minute^{-1}) for 30 minutes. The permeate water was collected in a volumetric flask. Pure water flux was determined using the formula

$$J_w = \frac{V}{t \times s} \qquad (4)$$

where V is the volume of water in ml passed through the membrane in time t minute and S is the effective area of the membrane (cm^{-1}).

2.4 Dye Rejection Experiments

A two-compartment membrane cell (Figure 1) was used for the study. Volume of each compartment of the cell was 50 ml. The polymeric membrane was placed between the compartments with silicone–rubber packing and the cell was connected with a reservoir of 500 ml. The aqueous solutions of the model compound was stirred continuously and circulated by peristaltic pump that was connected to the reservoir. Solutions of methyl green in the concentration ranging 0.01 to 0.05 mmole^{-1} were used for present work. The sample solutions were collected from the permeate side after a permeation period and analyzed by UV-VIS spectroscopy in an Analyticjena (Model: Specord 200) spectrophotometer. The measurements were made at the maximum wavelength (626 nm) in the visible range. The rejection percentage was defined as

$$R\% = \frac{C_f - C_p}{C_f} \times 100 \qquad (5)$$
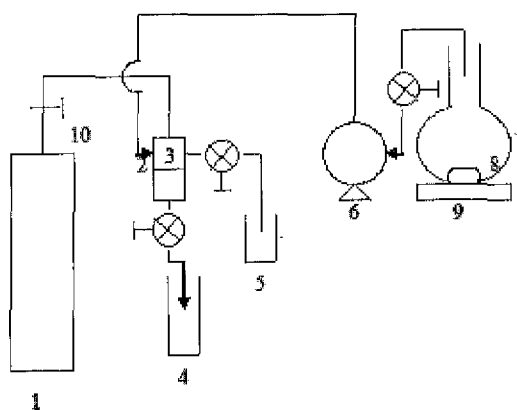
1. Nitrogen cylinder, 2. Membrane cell, 3. Membrane, 4. Collecting vessel, 5. Water tank, 6. Peristaltic pump, 7. Feed tank, 8. Magnetic niddle, 9. Magnetic stirrer, 10. Gas regulator

Figure 1 Diagrametric representation of the membrane cell

Table 2 Physical properties of the NF membrane

Parameter	Results
FTIR peak position (cm^{-1})	Assignment
3455	N-H stretching
2961	Aromatic C-H stretching
1600	Overlap of C=O stretching and amide
1585	C=C stretching
1488	C-N stretching
1298	Interaction between C-N stretching and N-H bending
Pore size range	13-71 nm
Porosity	59.6 %
Pure water permeability	3.40 x10^5 cmS^{-1} bar^{-1}

where C_f and C_p are the concentration in feed and permeate respectively in mmole L^{-1}.
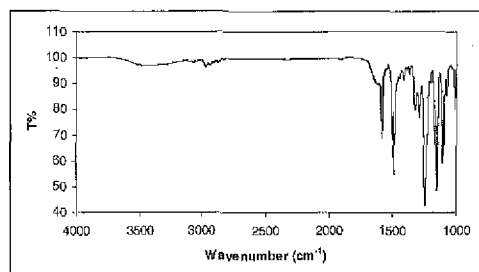
Figure 2   FTIR spectra of NF membrane

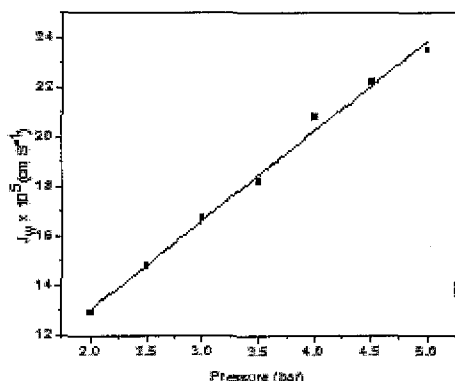**Figure 3**   SEM image of surface layer of NF membrane

Figure 4   The water flux of membranes at different operating pressure

3.0   RESULTS AND DISCUSSIONS

3.1   Characterization of Membrane

Figure 2, 3 and 4 show the FTIR spectra, SEM image of the membrane and the plot of J_w versus

Pressure (P) respectively. Amide and carboxylic group of the membrane was confirmed by the aborption bands The physical characteristic of the membrane evaluated from these analyses is listed in Table 2.

SEM photographs indicate that the membrane contains pores ofalmost similar shape but the pore diameters are not uniform. Surface roughness as visualized from SEM photographs seems to be low resulting in low fouling. The membrane is reported to exhibit a very thin skin layer of thickness 25 nm   as well as three layers in the membrane structure: a thin top layer of polyamide, an intermediate layer of polyethersulfone and a support layer of polyester [13].
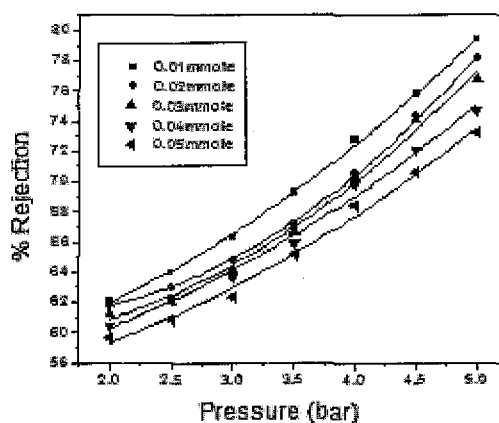

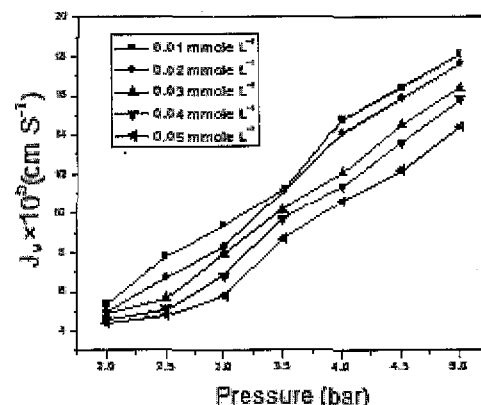**Figure 5**   Rejection of dye at different operating pressure

Figure 6   Variation of solvent flux with pressure at different dye concentration

3.2 Effect of Applied Pressure and Feed Concentration

The effect of applied pressure and dye concentration was studied at a range of pressure 2 bar to 5 bar and concentration range of 0.01 mmole L^{-1} and 0.05 mmole L^{-1}. Figure 5 shows the variation of percentage rejection as a function of pressure and concentration. The percentage rejection increases with increasing pressure and decreases with increase in concentrations an observation akin to that is reported for removal of other molecules and ions by nanofiltration [14]. The decrease in rejection with increasing concentration is marginal and may be attributed to cation shield effect [14] due to which membrane negatively charged groups became progressively stronger, leading to the decrease of membrane repulsive forces on the anions. Furthermore, with increase in pressure, convective transport becomes more important causing rejection to increase [14]. However, concentration polarization will also increase with increase of pressure which results in decrease in rejection. The counteracting contribution of increased convective transport and increased concentration polarization will result in nearly constant rejection at high pressure range [14].
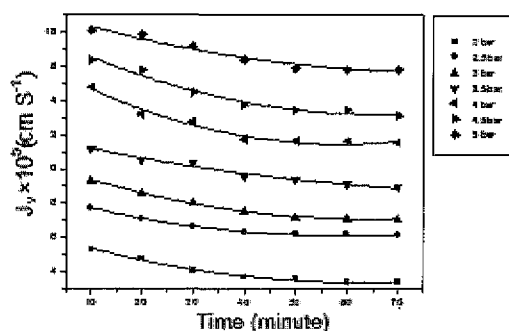

Figure 7 Variation of flux with time at different pressures at constant dye concentration of 0.01 mmole L^{-1}

3.3 Effect of Concentration Polarization on Permeate Flux

Figure 6 shows that the percentage rejection of the dye linearly increases with applied pressure indicating little or no effect of concentration polarization or fouling in the pressure range under study [12]. This may be due to the hydrophilicity of the membrane. NF 270-400 is hydrophilic in nature [15] and has better fouling resistance capacity than hydrophobic membrane [16]. Figure 7 shows that the decrease in permeate flux with time is insignificant. This implies that in the range of pressure studied, the membrane does not suffer much compaction effects which would reduce its pores and consequently the permeate flux [7].

3.4 Mechanism of Transport

In order to predict the effect of different parameters on flux and the rejection in nanofiltration of the dye solution, first, the effect of osmotic pressure was taken into account. The osmotic pressure of the methyl green solutions was determined using the Van't-Hoff equation [4] according to which

$$or, \Pi = \frac{nRT}{V} \tag{6}$$

where, Π is the osmotic pressure across the membrane, n is the number of moles of dye taken, R is the universal gas constant, T is the temperature at which experiment was performed and V is the volume of the dye solution taken. The nanofiltration permeation performance is shown in Figure 8 which shows the variation of J_v versus ΔP at different feed concentrations. The figure shows a considerable deviation of the experimental results from those calculated by the equation
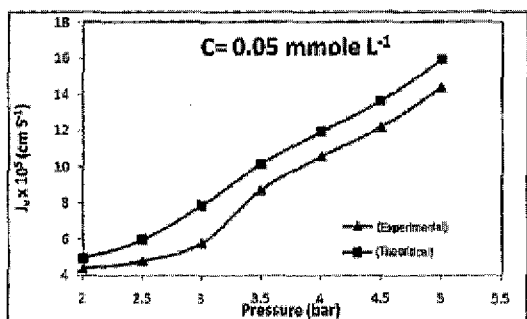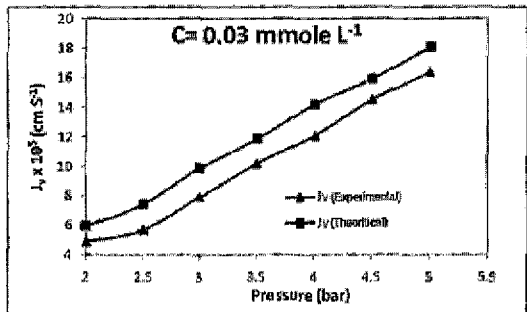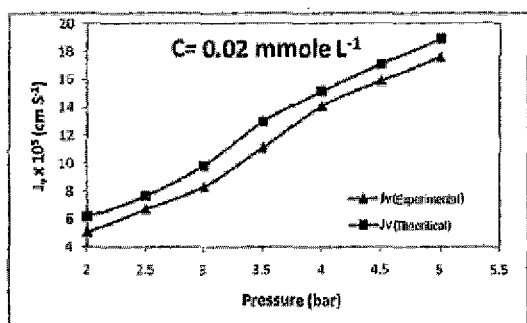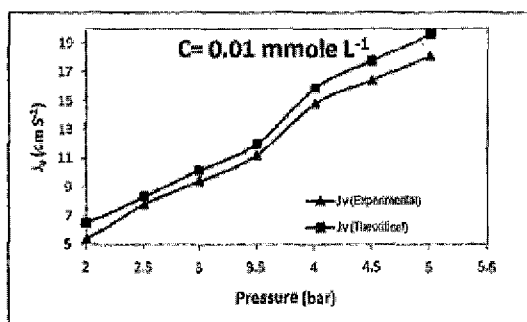
$$J_v = \frac{\Delta P - \Delta \Pi}{\mu R_m} \tag{7}$$

Table 3 Values of the water permeability co-efficient, L'_p and adsorption resistance, R_{ads}, obtained at several feed dye concentrations

C_f (mmole L^{-1})	$L'_p \times 10^{-5}$ (cm bar^{-1} Sec^{-1})	$R_{ads} \times 10^5$ (cm^{-1})
0.01	3.30	4.23
0.02	3.18	5.69
0.03	3.16	5.89
0.04	3.09	6.81
0.05	3.04	7.41

The intrinsic membrane resistance, R_m as obtained from the linear plot of J_w vs ΔP was 3.37×10^6 cm^{-1} in the pressure and concentration range under study. As the calculated and experimental results of the plot J_v versus ΔP shows deviation when only R_m is considered, resistances due to other factors such as concentration polarization (R_g) and adsorption (R_{ads}) should be taken into account. As mentioned earlier, effect of concentration polarization in this case is negligible. Earlier workers also have reported that effect of concentration polarization is not so significant [7, 14] in nanofiltration of dye molecules, but effect of adsorption plays an important role [4]. Therefore, adsorption resistance (R_{ads}) was evaluated and R_g was neglected in this study.
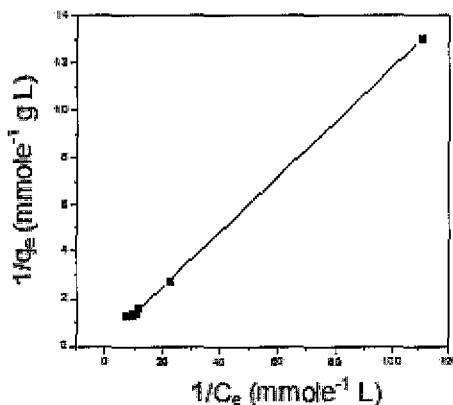

Figure 8 Theoretical and experimental flux vs pressure at different dye concentration

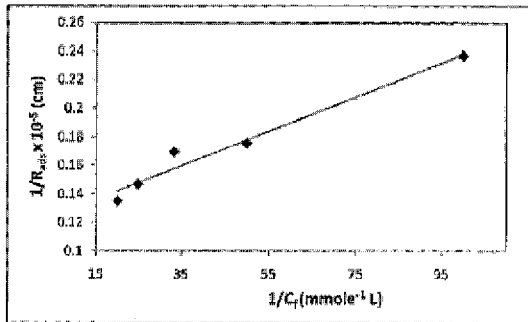**Figure 9** Langmuir plot for adsorption on NF membrane

Figure 10 Langmuir type plot of adsorption resistance vs dye concentration

In order to calculate R_{ads}, pure water permeability J_w was determined after permeation of dye of each concentration. The value of $L_p{}'$ was determined from the linear plot of J_w versus ΔP from which R_{ads} can be calculated. Table 3 represents the water permeability co-efficient, $L_p{}'$ and adsorption resistance, R_{ads} obtained at several feed dye concentration.

To study the adsorption behavior of the NF membrane, adsorption experiments were performed independently at a concentration range (0.01 to 0.25 mmole L^{-1}) and adsorption isotherms were determined (Figure 9). Values of co-relation co-efficients show that the present system better fits to the Langmuir model than Freundlich model. Adsorption process was also studied with respect to thermodynamic parameters. Negative value of Gibb's free energy of adsorption means that the adsorption of the dye on the membrane is thermodynamically favorable; moreover relatively low values of ΔG_{ads} indicate physical adsorption process [17].

Assuming that R_{ads} is proportional to amount of dye adsorbed per unit mass of the membrane, q, an equation, similar to Langmuir equation can be written as:

$$\frac{1}{R_{ads}} = \frac{1}{R_{max} \, bC_f} + \frac{1}{R_{max}} \qquad [8]$$

where R_{ads} is the adsorption resistance (cm^{-1}), R_{max} is the saturation value of adsorption resistance, C_f is the dye concentration (mmole L^{-1}) and b is adjustable parameter (mmole L^{-1}).
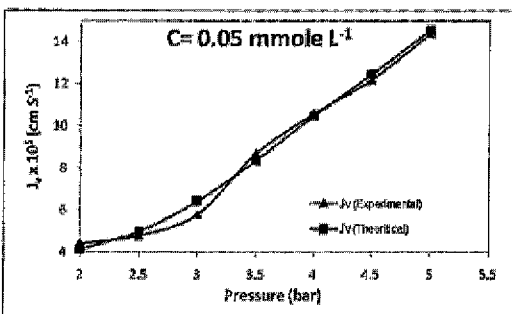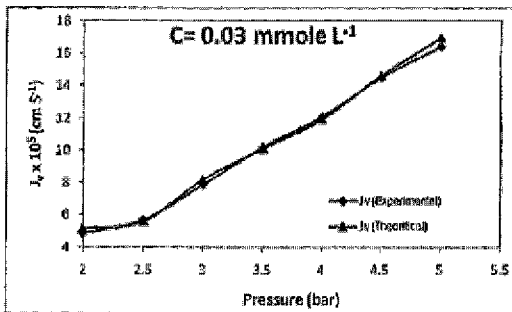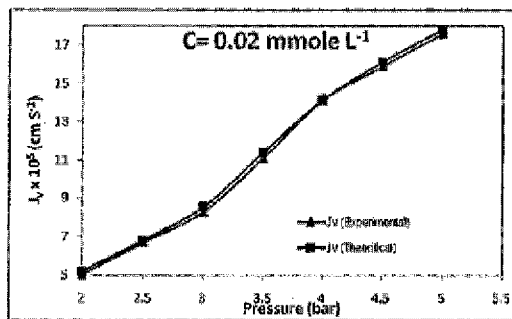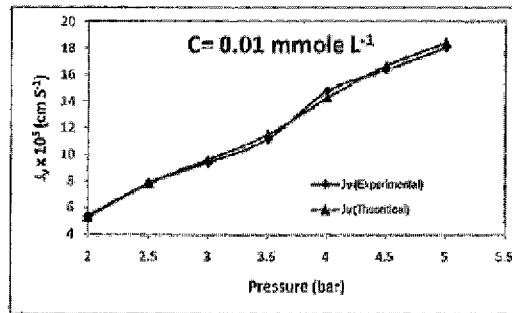

Figure 11 Flux vs pressure considering adsorption resistance

A Langmuir type plot can be obtained between C_f and R_{ads} (Figure 10). Including R_{ads} in equation 1, the permeate flux, J_v were then calculated. As shown in Figure 11, the experimental and calculated values now become almost equal. This shows that in case of permeation of dye through NF membrane, effect of adsorption should be taken into account. As documented in literature and our experimental results, this study also shows that effect of other factors such as concentration polarization does not have significant effect on permeation of dye through NF membrane as the experimental J_v values agree quite well to calculated J_v values considering only the intrinsic membrane resistance and adsorption resistance.

4.0 CONCLUSIONS

Nanofiltration membrane can provide an attractive method for removal of dye from its aqueous solution, which may be useful for treatment of dye effluents in textile and dye industries as well as for extraction of natural dye. Effect of applied pressure on rejection was found to be appreciable; the feed concentration seems to be less pronounced. The transport process is governed mainly by membrane resistance and that due to adsorption. The effect of concentration polarization has little effect on the permeation process. However, a detail investigation with a number of dye molecules will be necessary to draw a more precise conclusion on the mechanism of the transport in the NF membrane.

REFERENCES

[1]   EPA Order Huan-Shu-Shui-Tzu No. 0980065341 on July 28, 2009.

[2]   Wong, Y. C., Y. S. Szeto, W. H. Cheung and G. McKey. 2003. Equilibrium Studies for Acid Dye Adsorption onto Chitosan. *Langmuir*. 19: 7888-7894.

[3]   Lucia, R., P. Martin, H. Miroslav and J. Augustin. 2009. Sorption of Cationic Dyes from Aqueous Solutions by Moss Rhytidiadelphus Squarrosus: Kinetics and Equlibrium Studies. *Nova Biotechnologica*. 9-1: 53-61.

[4]   Gomes, A. C., I. C. Goncalves and M. N. de Pinho. 2005. The Role of Adsorption on Nanofiltration of Azo Dyes. *J. Membrane Sci*. 255: 157-165.

[5]   Akbari, A., J. C. Remigy and P. Aptel. 2002. Treatment of Textile Dye Effluent Using Polyamide-based Nanofiltration Membrane. *Chem. Eng J*. 41: 601-609.

[6]   Hassani, A. H., R. Mirzayayee, S. Nasseri, M. Borghei, M. Gholami and B. Torabifar. 2008. Nanofiltration Process on Dye Removal from Simulated Textile Wastewater. *IJESE*. 5(3): 401-408.

[7]   De Souza, A. A. U., J. C. C. Petrus, F. P. Santos, H. L. Brandao, S. M. A. G. U. Souza and L.N. Juliano. 2009. Colour Reduction in Textile Effluents by Membranes. *L.A.A.R.*. 39: 47-52.

[8]   Banerjee P., S. DasGupta and S. De. 2006. Removal of Dye from Aqueous Solution Using A Combination of Advanced Oxidation Process and Nanofiltration. 2007. *J. Hazard. Mater*. 140(1-2): 95-103.

[9]   Aseeri, M. A., Q. B. Ali, S. Haji and N. A. Bastaki. 2007. Removal of Acid Red and Sodium Chloride Mixtures from Aqueous Solutions Using Nanofiltration. *Desalination*. 206: 407-413.

[10] Aydiner; C, Y. Kaya, Z. B. Gonder and I. Vergili. 2010. Evaluation of Membrane Fouling and Flux Decline Related with Mass Transport in Nanofiltration of Tartrazine Solution. *J Chem Tech Biot*. 85:1229-1240.

[11] Chakraborty; S., B. C. Bag, S. Dasgupta, J. K. Basu and S. De. 2004. Prediction of

Permeate Flux and Permeate Concentration in Nanofiltration of Dye Solution. *Sep Purif Technol.* 35: 141-152.

[12] Tu; S. C., R. Varadarajan, W. Den and M. Pirbazari. 2008. Predictive Membrane Transport Model for Nanofiltration Processes in Water Treatment. *AIChE Journal.* 47:1346-1362.

[13] Boussu; K., J. De Baerdemaeker, C. Dauwe, M. Weber, K. G. Lynn, D. Depla, S. Aldea, I. F. J. Vankelecom, C. Vandecasteele and B. V. der Bruggen. 2007. Physico-Chemical Characterization of Nanofiltration Membranes. *ChemPhysChem.* 8:370-379.

[14] Murth; Z. V. P. and L. B. Chaudhari. 2008. Separation of Cadmium Ions and Estimation of Membrane Transport Parameters of a Nanofiltration Membrane. *Indian J. Chem. Technol.* 15: 107-112.

[15] Pontie; M, H. Dach, J. Leparc, M. Hafsi and A. Lhassani. 2008. Novel Approach Combining Physico-Chemical Characterizations and Mass Transfer Modelling of Nanofiltration and Low Pressure Osmosis Membranes for Brakish Water Desalination Intensification. *Desalination.* 221:174-191.

[16] Mo; J. S. H. Son, J. Jegal, J. Kim and Y. H. Lee. 2007. Preparation and Characterization of Polyamide Nanofiltration Composite Membranes with TiO_2 Layers Chemically Connected to the Membrane Surface. *J. Appl. Polym. Sci,* 105(3): 1267-1274.

[17] Morao; A. I. C., A. M. B. Alves and M. D. Afonso. 2006. Concentration of Clavulanic Acid Broths: Influence of the Membrane Surface Charge Density on NF Operation. *J. Membrane Sci.* 281:417-428.